Available online at www.sciencedirect.com
ScienceDirect
Magnetic Resonance Imaging 27 (2009) 1030–1038
MAGNETIC RESONANCE IMAGING

Neural activity-induced modulation of BOLD poststimulus undershoot independent of the positive signal

Sepideh Sadaghiani, Kâmil Uğurbil[1], Kâmil Uludağ*
MPI for Biological Cybernetics, 72076 Tübingen, Germany
Received 3 November 2008; revised 31 March 2009; accepted 4 April 2009

Abstract

Despite intense research on the blood oxygenation level-dependent (BOLD) signal underlying functional magnetic resonance imaging, our understanding of its physiological basis is far from complete. In this study, it was investigated whether the so-called poststimulus BOLD signal undershoot is solely a passive vascular effect or actively induced by neural responses. Prolonged static and flickering black-white checkerboard stimulation with isoluminant grey screen as baseline condition were employed on eight human subjects. Within the same region of interest, the positive BOLD time courses for static and flickering stimuli were identical over the entire stimulus duration. In contrast, the static stimuli exhibited no poststimulus BOLD signal undershoot, whereas the flickering stimuli caused a strong BOLD poststimulus undershoot. To ease the interpretation, we performed an additional study measuring both BOLD signal and cerebral blood flow (CBF) using arterial spin labeling. Also for CBF, a difference in the poststimulus period was found for the two stimuli. Thus, a *passive* blood volume effect as the only contributor to the poststimulus undershoot comes short in explaining the BOLD poststimulus undershoot phenomenon for this particular experiment. Rather, an additional *active* neuronal activation or deactivation can strongly modulate the BOLD poststimulus behavior. In summary, the poststimulus time course of BOLD signal could potentially be used to differentiate neuronal activity patterns that are otherwise indistinguishable using the positive evoked response.

Keywords: BOLD signal; fMRI; Post-stimulus undershoot; CBF; Arterial spin labeling

1. Introduction

Since its discovery [1–3], functional magnetic resonance imaging (fMRI) methodology based on blood oxygenation level-dependent (BOLD) contrast [4] has become the most important tool for mapping neuronal activity, especially in humans. The time course of this signal has been studied in great detail (for review, see Ref. [5]). Briefly, following sensory stimulation or execution of a behavioral task, the signal intensity detected in BOLD-weighted magnetic resonance (MR) images is altered after 1–2 s and reaches its maximum deviation from baseline after 5–10 s. An initial dip of the BOLD signal below baseline is observed in some experiments just after stimulation begins and prior to the large stimulus-evoked positive signal change (for an overview, see Refs. [6,7]). A few seconds after cessation of stimulation, the BOLD signal returns to baseline, often after a transient but robust poststimulus undershoot (Ref. [8] and references therein).

The BOLD signal poststimulus undershoot is a transient effect which suggests that cerebral blood flow (CBF), cerebral blood volume (CBV) occupied by deoxyhemoglobin, and/or cerebral metabolic rate of oxygen consumption ($CMRO_2$) deviate differentially from the baseline after the termination of stimulation [5]. Despite intense research, the mechanisms underlying this phenomenon are not completely understood. Three possible explanations have been proposed for this effect which are nonexclusive and can simultaneously contribute to the BOLD signal poststimulus time course:

1. *Higher deoxyhemoglobin content per voxel due to elevated deoxyhemoglobin-containing CBV*: Venous CBV containing most of the deoxyhemoglobin is postulated to return to baseline much more slowly than

* Corresponding author. Tel.: +49 7071 601 900; fax: +49 7071 601 702.
E-mail address: kamil.uludag@tuebingen.mpg.de (K. Uludağ).
[1] Current Address: Center for Magnetic Resonance Research, Minneapolis, USA.

0730-725X/$ – see front matter © 2009 Elsevier Inc. All rights reserved.
doi:10.1016/j.mri.2009.04.003

CBF due to the biomechanical properties of venous vessels (lack of smooth muscles around veins) [9,10].
2. *Persistent elevated oxygen metabolism*: CBF recovery to baseline is proposed to occur more rapidly than that of $CMRO_2$; that is, elevated oxygen consumption rate, originally induced by the stimulation, persists after stimulation has ended while the poststimulus oxygen delivery by CBF decreases to basal levels [11,12].
3. *Reduced delivery of oxygenated hemoglobin*: this hypothesis posits that CBF (and to a lesser extent $CMRO_2$) decreases *below* baseline after stimulus termination, possibly due to neuronal inhibition or reduction of the balanced excitation–inhibition activity in the poststimulus period [13–15].

There are fundamental and testable differences among these explanations. The first suggestion posits that the poststimulus undershoot is only a *passive* phenomenon that must bear a fixed relationship to the stimulus-induced positive BOLD signal level that precedes it. Thus, for the same stimulus-evoked positive BOLD response, it is expected that the venous CBV is elevated to the same level during the stimulus, consequently leading to the same poststimulus CBV kinetics and the same BOLD undershoot. If, however, for different stimuli different poststimulus responses were observed for the same positive BOLD effect the second and/or the third explanation given above would be favored. This case would indicate an *active* neuronal contribution to the poststimulus behavior of the BOLD signal either from $CMRO_2$ or CBF (or both). Note that this line of argumentation also assumes the ratio between CBF and $CMRO_2$ during stimulation to be the same for identical BOLD signal amplitude. Additional physiological measures, such as baseline CBF or CBF change during stimulation, can reveal whether same BOLD signal really implies identical set of changes of the underlying physiological parameter ($CMRO_2$, CBF, and CBV) (cf. Discussion section).

This hypothesis forms the basis of the present study. 180 s of visual stimulation with static and flickering black-white checkerboards were applied and the time course of the BOLD response examined. Extended duration visual stimulation has often been used to investigate fMRI signal dynamics [11,13,16]. Radial flickering checkerboards are potent stimuli to cause pronounced BOLD signal undershoots [13]. We chose to compare the response to flickering and static checkerboards because the difference in the induced poststimulus perceptual states might suggest a difference in poststimulus neuronal activation patterns. While for static checkerboards, a strong afterimage is perceptually reported this is not the case for flickering checkerboards. Thus, using different luminance contrasts for static and flickering checkerboards, we aimed to induce the same positive response and then to probe the poststimulus behavior of the BOLD signal. In order to further ease the interpretation of the BOLD data, the first experiment was repeated using the arterial spin labeling (ASL) technique, measuring CBF in addition to the BOLD signal.

2. Methods

2.1. Study design

A first experiment aimed at modulating the BOLD poststimulus undershoot independently of the positive BOLD time course. Two supplementary experiments in addition to this main experiment were performed. The second experiment measured CBF in addition to BOLD signal in order to disambiguate the interpretation of the findings. The third BOLD experiment further investigated the neural basis of this effect.

Eight healthy participants (two female, six male, age range: 22–34) took part in the first and third experiments. Four healthy subjects (one female, age range: 24–43) participated in the second experiment (CBF/BOLD signal) on a separate scanning session. One subject's data set had to be excluded from the second experiment because of exceptionally noisy CBF signal lacking a clear stimulus evoked positive response. All subjects gave informed consent according to procedures approved by the local ethics committee. Subjects were instructed to fixate on a white fixation square at the centre of the screen throughout each run.

2.2. Stimuli

In each of three experiments, we compared cortical responses to static and flickering checkerboards. Within each run, we used either static or flickering checkerboards. Experimental runs alternated between static and flickering checkerboard conditions. Flickering checkerboards reversed their pattern at 4 Hz (eight reversals per second). The baseline periods consisted of a grey display that was isoluminant with the mean luminance of the checkerboard, thereby avoiding abrupt luminance changes. Luminance was measured from the projection screen inside the MR scanner room using a luminance meter (Minolta chroma meter CS-100, Osaka, Japan).

2.3. First experiment

Full-field black-white radial checkerboards were used. In a prior pilot experiment on a few subjects we estimated the optimal luminance contrast between black and white checks for the flickering checkerboard in order to induce the same positive BOLD signal amplitude as found for a full-contrast static checkerboard. The resulting luminance contrast of the flickering checkerboard (Michelson contrast 1/3) was lower compared to the static checkerboard (Michelson contrast 1) (Fig. 1). After an initial 60 s baseline period of grey display, each run consisted of two repetitions of 180 s checkerboard

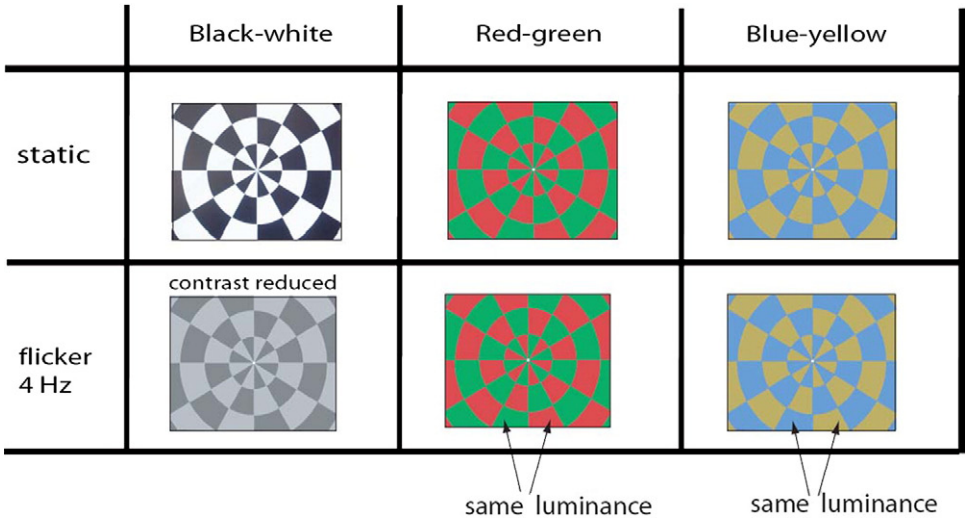

Fig. 1. Stimuli. Radial checkerboards were presented either in a static or flickering (4 Hz) fashion. In experiment 1 (fMRI) and experiment 2 (ASL) black-white checkerboards were used while experiment 3 (fMRI) made use of red-green and blue-yellow checkerboards with isoluminant checks. After an initial baseline the stimuli were shown for 180 s followed by 150 s of baseline.

stimulation followed by 150 s of grey display resulting in a total duration of 720 s per run.

2.4. Second experiment (ASL)

Stimuli were identical to experiment 1 except that each run consisted of one instead of two repetitions of the stimulus; 120 s of initial baseline was followed by 180 s of black-white checkerboard stimulation and a final 150 s of poststimulus grey display.

2.5. Third experiment

Full-field blue-yellow and red-green radial checkerboards were used. They were characterized by high color contrast but zero luminance contrast, i.e., the two colors were isoluminant (red matched green and blue matched yellow in luminance). Consequently, in contrast to the first experiment (black-white), luminance contrast was not different between static and flickering checkerboards (Fig. 1). Stimulus timing was identical to Experiment 1.

2.6. Data acquisition

Following a localizer scan, BOLD images were acquired on a 3T Siemens MAGNETOM Trio Tim Scanner (Siemens Medical Solutions, Erlangen, Germany). We applied a gradient echo-planar sequence with the following parameters: TR=1000 ms; TE=40 ms; flip angle=60°; FOV=240×240 mm^2; voxel size=3.75×3.75×3 mm^3. Twelve oblique slices covering early visual areas were acquired. Six functional runs of 720 TRs' length (one run for static and one for flicker stimuli for black-white, red-green and blue-yellow, respectively) were acquired in a single session. For the second experiment, CBF and BOLD signals were measured using a PICORE-Q2TIPS ASL (Arterial Spin Labeling) sequence [17] with the following standard parameters: TR=2000 ms, TE=16 ms, flip angle=80°, FOV=256×256 mm^2; voxel size=4×4×4 mm^3, TI1=700 ms, TI1s=1200 ms, TI2=1400 ms. Nine oblique slices covering early visual areas were acquired. In order to overcome the relatively low signal-to-noise ratio of CBF measurements, four runs of static and four runs of flickering black-white checkerboards were conducted. Hence, eight runs of 225 TRs' length were acquired.

2.7. Data analysis

Extraction of signal time course was carried out in two steps and for each subject separately. First, standard statistical methods were employed to select a set of early visual cortex voxels that were active for static as well as flickering stimuli. Next, raw BOLD time courses from the voxels that were selected in the first step were extracted. Note that time courses for static and flickering conditions were extracted from one and the same set of voxels.

The statistical analysis was carried out using the FSL software library (http://www.fmrib.ox.ac.uk/fsl) [18]. Motion-correction was performed for each run using *mcflirt* and the static and flickering checkerboard data were co-registered using *Flirt* [19]. Data were analyzed using the general linear model with *Feat* for each run utilizing default impulse hemodynamic response function [20]. Parameter estimates of the first-level analyses for static and flickering checkerboards were entered into a within-subject mixed-effects analysis [21]. This procedure allows the specification of the voxels that were most active for *both* static and flickering checkerboard conditions. The resulting *z*-statistical maps were thresholded on a subject-by-subject basis for extraction of the 50, 100 or 150 most active voxels (average mixed-effects z-threshold of 1.83, 1.74 and 1.66 for black-white (first experiment), 1.84, 1.75 and 1.68 for blue-yellow and 1.86, 1.78 and 1.71 for red-green (third experiment),

respectively). In the second step, the BOLD time courses of these voxels were averaged for each subject across the selected voxels and across both repetitions in each run. The baseline signal levels for percentage change calculations were defined as the average signal value during the final 30 s of the grey display period from both stimulus repetitions. No detrending or high-pass filtering was used. The effects were robust even if detrending was used (data not shown).

For demonstration purposes, an additional general linear model was set up with a second regressor modelling the poststimulus period (30 s) in addition to the regressor for the stimulation period. A within-subject fixed effects analysis across static and flicker sessions was performed on the poststimulus regressor. Fig. 2C shows representative results for a single subject.

For the second experiment using ASL, voxel time courses were extracted in a similar way as for the first experiment: a general linear model for each run modelled CBF as well as BOLD signal. First-level results were entered into within-subject mixed-effects analyses. Again, 50, 100 or 150 activated voxels, based on BOLD signal statistical maps, were selected for extraction and averaging of the CBF and BOLD signal time courses. The BOLD time course was extracted as the average between control and tag measurements, and the CBF time course, as the difference between control and tag measurements [22]. Because control and tag images are acquired with a time lag of one TR, the control and tag time courses were linearly interpolated to double the time resolution in order to construct difference and average time courses using the appropriate time points, thereby reducing the BOLD signal contamination of the CBF data [22]. The baseline signal levels for percentage change calculations were defined as the average signal value during 90 s of the grey display period before stimulus onset. To reduce noise, CBF data were smoothed using a sliding temporal window average of 10 data points.

To test for statistically significant differences between responses to static and flickering stimuli the signal from the poststimulus time window and two comparable steady-state time windows were entered into two-way analyses of variance (ANOVAs) with the factors condition (static vs. flicker) and temporal window (three 30 s windows). The signal was averaged across the 30 s of each window. The windows were 60–90 s, 150–180 s (i.e., last 30 s of stimulation) and 195–225 s (i.e., undershoot) relative to stimulus onset at 0 s.

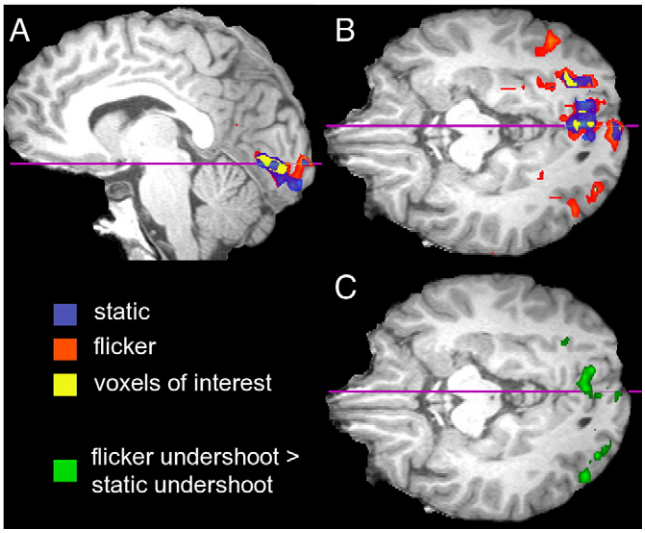

Fig. 2. Illustration of voxel selection and undershoot effect for a single representative subject for the first experiment (BOLD imaging of black-white checkerboard stimulation). (A and B) Positive evoked responses to sustained static (blue) and 4-Hz flickering (orange) checkerboard stimulation (threshold P=.0001 uncorrected). The responses largely overlap and include some additional activation foci for flickering stimuli most prominently in MT+. The 100 voxels most significantly responding to both static and flickering stimuli (yellow) were selected for time course extraction on a subject-by-subject basis. (C) The poststimulus undershoot was modeled by a second regressor and contrasted for flicker vs. static (green). The undershoot difference is largely confined to areas that showed a positive response and overlaps with the voxels selected for time course extraction. The reverse contrast is overlayed here, but didn't yield significant voxels (same slice as B; threshold P=.001 uncorrected). The purple lines indicate the position of the slices displayed in horizontal or sagittal views, respectively.

3. Results

3.1. Perceptual reports

After the scanning sessions, all subjects reported the perception of after-images for all experiments (1-3). Static stimuli caused a strong after-image of a sharp and clear checkerboard with a subjectively estimated duration of 1 to 2 min. The after-images following colored static stimuli were described to have inverted or novel colors. Flicker stimuli induced a substantially weaker after-image of few seconds duration described as a blurry image of the edges between the checks resembling a spider's web.

3.2. Functional imaging results

Voxels for time course analysis were selected on a subject-by-subject basis. Fig. 2A/B demonstrates this process for a representative subject for experiment 1. Voxels most significantly responding to both flickering and static stimuli were defined in a within-subject second-level analysis. Thus, the same set of voxel served for time course extraction for static and flickering stimuli. These voxels were located in early visual cortices most prominently in V1 in the calcarine fissure. For demonstration purposes, a second general linear model was calculated including an additional regressor for the poststimulus period. Fig. 2C demonstrates the spatial pattern of the difference in undershoot between flicker and static stimuli for the same subject.

The raw BOLD signal time course was extracted for each subject from the selected voxels. Fig. 3 shows BOLD time courses as averaged across subjects (8 subjects, 100 most active voxels, 6 runs, 2 repetitions per run). For all three color pairs (Experiments 1 and 3), the static and flickering stimuli

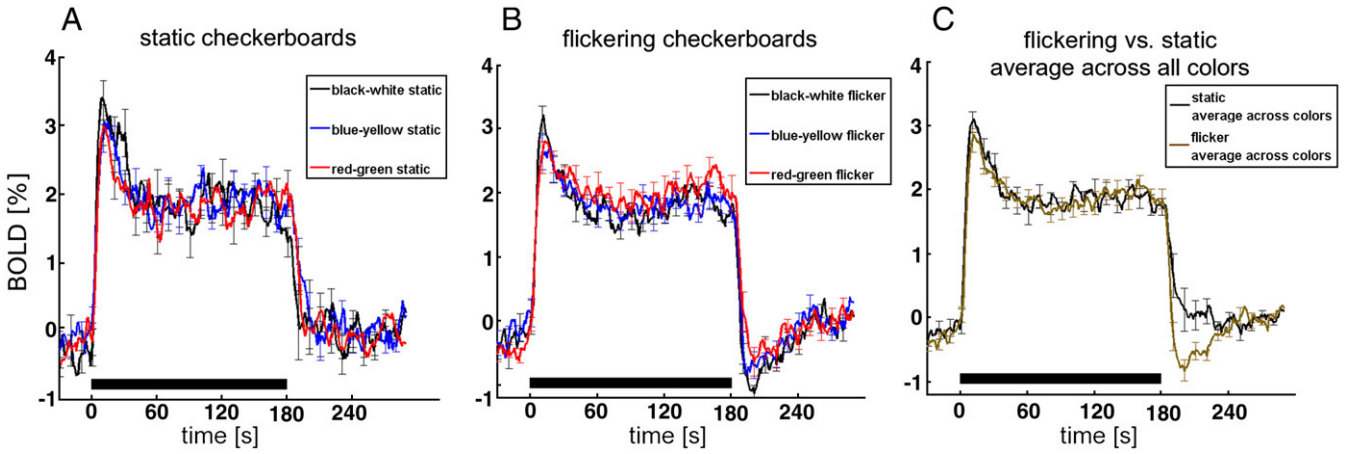

Fig. 3. BOLD time courses from Experiments 1 and 3. Curves are averaged across subjects (8 subjects, 100 most active voxels, 6 runs, 2 repetitions per run) for static stimuli (A), flickering stimuli (B) and average of all static vs. all flickering stimuli (C). Although the BOLD responses have very similar time courses (initial overshoot and adaptation to steady-state) and amplitudes during stimulation, the flickering stimuli exhibit a much larger decrease in BOLD signal after stimulation than the static stimuli. Error bars (for every 10th volume) indicate±S.E.M.

resulted in almost identical positive BOLD time courses during stimulation (Fig. 3A–C). After an initial overshoot of similar magnitude, the BOLD signal attained the same steady-state level for both conditions. Exact values for the initial overshoot (average of 8–12 s after stimulus onset) were black-white static: 3.3±0.7% and flicker: 3.0±0.5%; blue-

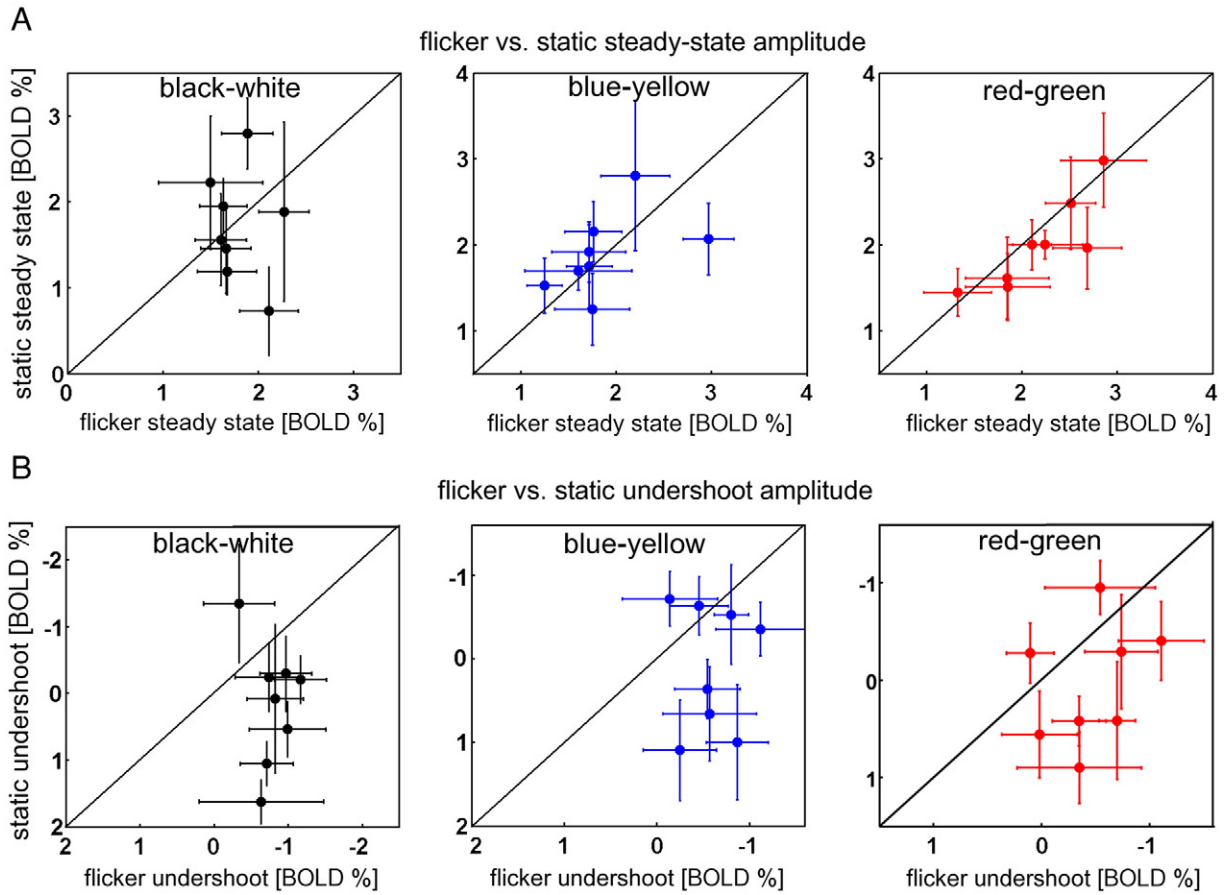

Fig. 4. Individual subjects' data from experiments 1 and 3. (A) Steady-state amplitudes (average of the last 30 s of the stimulation period with ±S.D.). (B) poststimulus amplitudes (average of 30 s beginning 15 s after stimulus offset with ±S.D.) for static vs. flickering stimuli shown for each subject. During steady-state, each subject has similar values for flickering and static stimulation. However, the poststimulus BOLD signal deviates much more from baseline for flickering than for static stimulation. Note that for better visualization the scales are inverted in (B).

yellow static: 2.8±0.8% and flicker: 2.5±0.8%; red-green static: 2.9±0.8% and flicker: 2.5±0.6%. Exact values for the steady-state level (average of 60–120 s after stimulus onset) were: black-white static 1.8±0.5% and flicker: 1.7±0.3%; blue-yellow static: 1.9±0.4% and flicker: 1.8±0.5%; red-green static: 1.8±0.5% and flicker: 2.0±0.5%. The time courses averaged across all colors of Experiment 1 and 3 (Fig. 3C) were surprisingly well matched during the stimulation period.

In contrast, the signal after stimulus cessation differed considerably between static and flickering conditions. A poststimulus undershoot was observed for the *flickering* stimulus (black-white: −1.0±0.4%; blue-yellow: −0.7±0.5%; red-green: −0.6±0.6%; for 20–24 s after stimulus offset), while the *static* stimuli caused no undershoot (black-white: 0.14±1.4%; blue-yellow static: 0.1±1%; red-green static: 0±0.8%). The maximum negative value for the average of the three flickering checkerboards was −0.95%, which is approximately 50% of the steady-state value during stimulation.

Fig. 4 shows results for all individual subjects (N=8). As shown in Fig. 4A, the steady-state amplitudes (average of the last 30 s of stimulation) for the flickering versus the static stimuli were distributed along the identity line for individual experiments. This shows that subjects with a large BOLD response to one stimulus also had a large response to the other stimulus and that the steady-state amplitudes were not substantially different for the static and flickering conditions. In contrast, during the poststimulus period signal amplitudes were for most subjects more negative for flickering than for static stimuli (Fig. 4B).

Statistical significance and specificity of this effect was tested for experiment 1 using a two-way ANOVA with the factors *condition* (two levels: static and flicker) and *temporal window* (three levels: average signal from three separate 30-s time windows). The time windows included the poststimulus time (beginning 15 s poststimulus to account for BOLD delay and allow undershoot to begin) and two comparable windows during the steady state positive response (1–1.5 min after stimulus onset and the last 30 s of stimulation). The ANOVA revealed a main effect of temporal window ($F_{1.2,8.3}$=136.7; P<.0001) and most crucially an interaction between temporal window and condition ($F_{1.3,9.2}$=12.6; P=.004). Post hoc paired t tests revealed significantly larger undershoot for flicker in the poststimulus time window (t_7=2.7, P=.03) but were not significant in the two steady-state time windows.

In the second experiment where changes in CBF using the ASL technique were measured, we could reproduce the above-described observations on the BOLD response also for CBF signals (n= 3), namely, the poststimulus undershoot was different despite the same positive response to flickering *versus* static stimuli (Fig. 5). A small poststimulus undershoot in CBF for the flickering condition was observed while the positive CBF signal declined to baseline slowly for the static condition after the stimulus ended. This pattern was

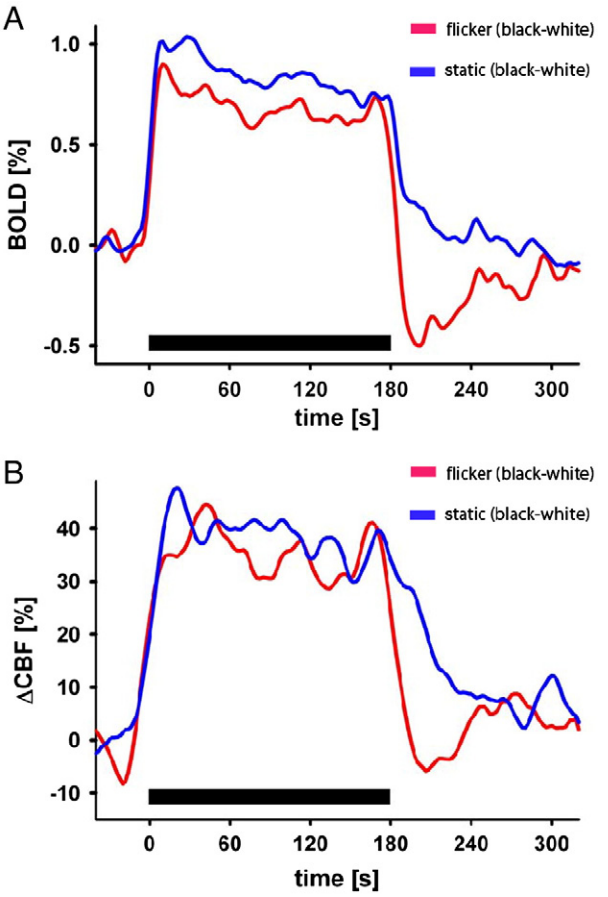

Fig. 5. Results of experiment 2 using arterial spin labeling. Average BOLD signal (A) and CBF (B) time courses (three subjects, eight runs each, 100 most active voxels) for static and flickering black-white checkerboard stimulation. Results for the BOLD signal reproduced the results of the first experiment shown in Fig. 3. CBF recovered to baseline more slowly after stimulation with static than with flickering stimuli.

clearly and consistently expressed in the individual data of all three subjects. The BOLD poststimulus undershoot for flickering checkerboard relative to the positive BOLD response dipped much further below baseline than the analogous effect observed for CBF.

For Experiment 3, the equivalent 2-way ANOVAs replicated the above results for colored checkerboards and revealed main effects of temporal window (blue-yellow: $F_{1.3,8.8}$=163.8; P<.0001, red-green: $F_{1.5,10.7}$=176.9; P<.0001) and, importantly, interactions between temporal window and condition (blue-yellow: $F_{1.4,10.1}$=5.8; P=.03 red-green: $F_{1.4,10.0}$=5.6; P=.03). Post hoc paired t tests again revealed significantly larger undershoots for flicker in the poststimulus time window (blue-yellow: t_7=2.4, P=.04, red-green marginally significant: t_7=2.3, P=.05 two-sided), while there were not significant in the two steady-state time windows.

All results presented were constructed from the 100 most active voxels. Changing the number of voxels (to 50 or 150 most active voxels) included in the analysis yielded

highly similar time courses with matched positive BOLD responses and larger undershoots for flickering checkerboards (data not shown).

4. Discussion

Mass neuronal activity patterns can currently be assessed only by measurement techniques integrating activity of many neurons. For example, local field potentials (LFP) are sensitive, among other things, to excitatory or inhibitory postsynaptic potentials from populations of neurons having a point-spread-function (PSF) of at least 0.5 mm around the electrode tip [23]. As another example, the BOLD signal which is sensitive to tissue oxygen metabolism, cerebral blood flow and volume has a minimal PSF of 1 mm^3 [24]. In such volumes of human brain tissue, there are more than 10^4 neurons [25,26]. As a consequence, during sensory stimulation or behavioral tasks, different neuronal activity patterns can potentially give rise to the same measured signal.

Responses of single neurons and neuronal populations may not only differ during stimulation but also after stimulation, e.g., due to an off-response excitation, post-stimulus inhibition or recovery to baseline level with different time constants [27–30]. Thus, temporal characteristics of the BOLD signal and also other techniques can be used as a tool to probe neuronal activity patterns that might generate indistinguishable results during steady-state. In this study, poststimulus behavior of neuronal activity was exploited using fMRI.

It was found that although the positive BOLD response was matched for static and flickering checkerboard stimulation, the poststimulus undershoot was significantly larger for the flickering checkerboards within one and the same voxel set. Could, in the current study, vascular effects be responsible for the different poststimulus time courses observed? Typically, differences in BOLD signal during stimulation are interpreted as differences of the underlying neuronal activity. Likewise, same BOLD signal is considered to be caused by the same neuronal activity. However, if the neurovascular coupling differs for two brain areas or for a brain area for different stimuli, then these interpretations might not be correct. The BOLD signal amplitude is influenced by the amount of deoxygenated hemoglobin during baseline and by the ratio of the changes in CBF and $CMRO_2$ (Ref. [5] and references therein). Thus, additional physiological measures are needed to disambiguate the BOLD signal amplitude. In our study, the CBF measurement served this purpose. Because CBF and BOLD signal during stimulation were identical for flickering and static conditions and because CBF and CBV are causally linked by the blood vessel properties (Ref. [31] and references therein), it is safe to conclude that the venous CBV elevation during stimulation was also the same. We note as an aside, however, that to the best of our knowledge the relationship of CBF and total or venous CBV has not been systematically investigated. Furthermore, the results were obtained by averaging the responses of one and the same set of voxels which were active for both stimuli. The use of same voxels for analysis ensured that voxels with the same underlying vasculature were averaged and compared. Inflow effects are not likely to play a role as the observed BOLD signal undershoot differences are robust for the two experiments (experiment 1: TR=1000 ms, experiment 2: TR=2000 ms).

Mandeville et al. [9] have shown that CBV elevation induced during the stimulation is followed by a slow CBV recovery after stimulus termination ("balloon effect" of venous vessels [8]). This balloon effect is likely operative in both types of stimuli used in our study. This implies that the poststimulus differences observed in our data cannot be explained solely by a passive biomechanical effect of blood vessel volume. In addition, perceptual after-effects were more expressed for static than for flickering stimuli indicating a differential neuronal poststimulus time course. Although it cannot be proven definitely, the differences that were observed in BOLD and CBF signals between static and flickering stimuli can most likely not be attributed to differences in vascular composition but are neuronal in origin.

The concurrent ASL study, where both CBF and the BOLD signal were measured, suggest that the differences in BOLD poststimulus time courses are caused largely, although not necessarily completely, by differences in oxygen delivery through CBF. That is, if CBF recovers fast while venous CBV recovers slow to baseline then a BOLD signal poststimulus undershoot is obtained; if, however, there is no large temporal mismatch between recovery of CBF and venous CBV to their respective baseline values, the BOLD undershoot is reduced or even not present. Note that although interpretation of our data does not require an "uncoupling" of $CMRO_2$ and CBF after the termination of the stimulation [11,12], an additional contribution from this effect cannot be ruled out.

4.1. Neuronal basis of the effect

Because CBF is closely associated with neural activity [14,32,33], the difference in CBF poststimulus time course presumably reflects a difference in neuronal activity. Since no electrophysiological data was obtained in this study, we can only speculate about the neuronal origin of the observed effects. A deviation of the CBF from baseline after stimulus cessation might be caused either by an off-response or by reduced neuronal activity. In the post-stimulus period after static stimulation, both BOLD signal and CBF returned to baseline slowly, with the latter displaying a slower decline. This behavior might be caused by activation of the so-called phasic neurons (see e.g., Refs. [27–29]) when the static stimulus is turned off or by sustained neuronal activation due to a visual after-effect either at the level of the retina or the visual cortex. The latter possibility receives support from our subjects' perceptual reports of a strong and long-lasting afterimage at offset of static checkerboards. If the neuronally caused slow recovery of CBF occurs on a long time scale

then there will be, as argued above, reduced temporal mismatch between recovery of CBF and venous CBV to their respective baseline values. That is, such an off-response counteracts the passive venous CBV-induced negative effects in the BOLD response for static checkerboards and explains why for static stimuli essentially no BOLD undershoot was observed. This finding has the important implication that the return of a BOLD signal to baseline — while CBF still deviates from baseline — does not necessarily mean that neuronal activity has also returned to baseline. Particularly, when using fast event-related stimulus paradigms, altered brain states during the experiment might not be visible in the BOLD signal because of insufficient time for neuronal activation to recover to baseline.

Additionally, neural mechanisms are likely to contribute to the BOLD signal and CBF decline below baseline after offset of flickering stimuli. A suppression of LFP in the early visual cortex after the stimulation period is frequently observed (see e.g., Ref. [14]). Considering the close association between oxygen metabolism and local field potentials [32,33], a neuronal poststimulus deactivation and, hence, a $CMRO_2$ and a coupled larger CBF reduction leads to hypo-oxygenation of blood. Such a mechanism would explain a CBF poststimulus deactivation [13,15] and an increased BOLD undershoot for the flickering stimuli used in this study. Note that because the origin of reduced CBF and $CMRO_2$ is neuronal deactivation and not the properties of the blood vessels, the reduced CBF after stimulus cessation should not be designated CBF undershoot but is better termed CBF poststimulus deactivation.

In contrast to previous findings and suggestions [13,16], the BOLD signal undershoot differences were observed for colored as well as for black-white high-spatial contrast stimuli. Hoge et al. [13] showed that the poststimulus undershoot amplitude can depend on the stimulus type. They suggested that the unique transient responses that they found for high-contrast flickering checkerboards were caused by magnocellular cells because these are mainly responsive to high luminance contrast. However, by using black-white stimuli of high luminance contrast as well as colored stimuli of isoluminant checks, we could show that the poststimulus undershoot was independent of luminance contrast. Bandettini et al. [16] showed no BOLD undershoot for diffuse-red flickering stimuli of 6 min duration but an undershoot for flickering black-white pinwheel stimuli. Clearly, more work has to be done — if possible together with electrophysiology — to ascertain the cause of these partially conflicting findings (e.g., spatial and temporal frequency of the stimuli, baseline luminance levels, stimulus duration, attentional load, voxel selection, magnetic field strength, MR sequence, etc.).

4.2. Conclusions and implications

The origin of the BOLD poststimulus undershoot is still a matter of debate. In the literature, the BOLD signal poststimulus time course has been attributed either to a passive vascular or to an active neuronal mechanism (e.g., Refs. [9–15]). We, however, have shown that an active, neurally driven component can considerably contribute to the so-called BOLD poststimulus time course *in addition to* a passive vascular effect ('balloon-effect'). This was demonstrated by the use of two different but related stimuli yielding the same stimulus-evoked BOLD and CBF responses during the stimulus period but differing in the post-stimulation period. The poststimulus undershoot should thus be understood as a phenomenon that goes beyond a passive biomechanical "balloon" effect. This finding contributes to our understanding of the mechanisms underlying the BOLD poststimulus time course.

In summary, different neurons or the same neurons to different extents are involved in processing static and flickering stimuli in the early visual cortex leading — most likely — to a sustained activity (static) and respectively to neuronal inhibition (flicker) after stimulus cessation. The poststimulus undershoot thus provides additional information on the underlying neural activation pattern beyond what a passive biomechanical "balloon" effect would suggest. In fact, in a recent review on adaptation fMRI [34], Krekelberg et al. [35] suggest that differences in BOLD signal poststimulus undershoot might reflect the number of activated cells or their differential involvement in the processing of the stimuli.

Importantly, we suggest that the BOLD poststimulus time course can potentially be utilized to differentiate neuronal activity patterns within a voxel in a manner beyond the capabilities of standard fMRI analogously to the adaptation fMRI approach [35]. We used a prolonged stimulation of 180 s to enhance the differential effect after stimulus cessation. However, because both neuronal effects described above can occur on much shorter time scales, it is also possible to perform similar experiments with shorter stimulus durations. Limitations are only posed by experimental signal-to-noise ratios and the temporal width of the impulse response function.

In conclusion, our findings indicate that neuronal activity contributes actively to the BOLD signal time course after stimulation cessation. Because differences in neuronal activity patterns taking place below the physiological and physical spatial resolution of the assay methodology and with no net change during stimulation is not directly detectable, we propose that the inspection of poststimulus signal behavior might be useful generally also for stimuli exploring other modalities. Using appropriate stimuli, the active undershoot component can potentially be applied to resolve functional neural organization and patterns of activity beyond the possibilities of standard fMRI and other neuroscience techniques sensitive to mass neuronal activity.

Acknowledgments

We thank Drs. Essa Yacoub, Nikos K. Logothetis and Gregor Rainer for helpful comments on the data and an earlier version of the manuscript.

References

[1] Bandettini PA, et al. Time-course spin-echo and gradient-echo EPI of the human brain during a breath hold. Proc., SMRM; 1992. Berlin.

[2] Kwong KK, et al. Dynamic magnetic resonance imaging of human brain activity during primary sensory stimulation. Proc Natl Acad Sci U S A 1992;89(12):5675–9.

[3] Ogawa S, et al. Intrinsic signal changes accompanying sensory stimulation: functional brain mapping with magnetic resonance imaging. Proc Natl Acad Sci U S A 1992;89(13):5951–5.

[4] Ogawa S, et al. Brain magnetic resonance imaging with contrast dependent on blood oxygenation. Proc Natl Acad Sci USA 1990;87: 9868–72.

[5] Buxton RB, et al. Modeling the hemodynamic response to brain activation. Neuroimage 2004;23(Suppl 1):S220–33.

[6] Ugurbil K, et al. Magnetic resonance studies of brain function and neurochemistry. Annu Rev Biomed Eng 2000;2:633–60.

[7] Buxton RB. The elusive initial dip. Neuroimage 2001;13(6 Pt 1): 953–8.

[8] Buxton RB, Wong EC, Frank LR. Dynamics of blood flow and oxygenation changes during brain activation: the balloon model. Magn Reson Med 1998;39:855–64.

[9] Mandeville JB, et al. Evidence of a cerebrovascular post-arteriole Windkessel with delayed compliance. J Cereb Blood Flow and Metabol 1999;19:679–89.

[10] Yacoub E, et al. The spatial dependence of the poststimulus undershoot as revealed by high-resolution BOLD- and CBV-weighted fMRI. J Cereb Blood Flow Metab 2006;26:634–44.

[11] Frahm J, et al. Dynamic uncoupling and recoupling of perfusion and oxidative metabolism during focal activation in man. Magn Reson Med 1996;35:143–8.

[12] Lu H, et al. Sustained poststimulus elevation in cerebral oxygen utilization after vascular recovery. J Cereb Blood Flow Metab 2004;24 (7):764–70.

[13] Hoge RD, et al. Stimulus-dependent BOLD and perfusion dynamics in human V1. Neuroimage 1999;9(6 Pt 1):573–85.

[14] Logothetis NK, et al. Neurophysiological investigation of the basis of the fMRI signal. Nature 2001;412(6843):150–7.

[15] Uludag K, et al. Coupling of cerebral blood flow and oxygen consumption during physiological activation and deactivation measured with fMRI. Neuroimage 2004;23(1):148–55.

[16] Bandettini PA, et al. Characterization of cerebral blood oxygenation and flow changes during prolonged brain activation. Human Brain Mapping 1997;5:93–109.

[17] Luh WM, et al. QUIPSS II with thin-slice TI1 periodic saturation: a method for improving accuracy of quantitative perfusion imaging using pulsed arterial spin labeling. Magn Reson Med 1999;41(6): 1246–54.

[18] Smith SM, et al. Advances in functional and structural MR image analysis and implementation as FSL. Neuroimage 2004;23(Suppl 1): S208–19.

[19] Jenkinson M, Smith S. A global optimisation method for robust affine registration of brain images. Med Image Anal 2001;5(2): 143–56.

[20] Woolrich MW, et al. Fully Bayesian spatio-temporal modeling of FMRI data. IEEE Trans Med Imaging 2004;23(2):213–31.

[21] Woolrich MW, et al. Multilevel linear modelling for FMRI group analysis using Bayesian inference. Neuroimage 2004;21(4): 1732–47.

[22] Wong EC, Buxton RB, Frank LR. Quantitative imaging of perfusion using a single subtraction (QUIPSS and QUIPSS II). Magn Reson Med 1998;39:702–8.

[23] Logothetis NK, Wandell BA. Interpreting the BOLD signal. Annu Rev Physiol 2004;66:735–69.

[24] Bolan PJ, et al. In vivo micro-MRI of intracortical neurovasculature. Neuroimage 2006;32(1):62–9.

[25] Haug H. Brain sizes, surfaces, and neuronal sizes of the cortex cerebri: a stereological investigation of man and his variability and a comparison with some mammals (primates, whales, marsupials, insectivores, and one elephant). Am J Anat 1987;180(2):126–42.

[26] Rockel AJ, Hiorns RW, Powell TP. The basic uniformity in structure of the neocortex. Brain 1980;103(2):221–44.

[27] Wang X, et al. Sustained firing in auditory cortex evoked by preferred stimuli. Nature 2005;435(7040):341–6.

[28] Detari L, Rasmusson DD, Semba K. The role of basal forebrain neurons in tonic and phasic activation of the cerebral cortex. Prog Neurobiol 1999;58(3):249–77.

[29] Ferraina S, Pare M, Wurtz RH. Disparity sensitivity of frontal eye field neurons. J Neurophysiol 2000;83(1):625–9.

[30] Uludag K. Transient and sustained BOLD responses to sustained visual stimulation. Magn Reson Imaging 2008;26(7):863–9.

[31] Weber B, et al. The microvascular system of the striate and extrastriate visual cortex of the macaque. Cereb Cortex 2008;18(10):2318–30.

[32] Attwell D, Iadecola C. The neural basis of functional brain imaging signals. Trends Neurosci 2002;25(12):621–5.

[33] Lauritzen M. Relationship of spikes, synaptic activity, and local changes of cerebral blood flow. J Cereb Blood Flow Metab 2001;21 (12):1367–83.

[34] Grill-Spector K, Malach R. fMR-adaptation: a tool for studying the functional properties of human cortical neurons. Acta Psychol (Amst) 2001;107(1-3):293–321.

[35] Krekelberg B, Boynton GM, van Wezel RJ. Adaptation: from single cells to BOLD signals. Trends Neurosci 2006;29(5):250–6.